

## Effect of Different Carbon Sources on Electrochemical Performance of LiFePO<sub>4</sub>/C

Cunsi Sun, Zheng Zhang, Mingming Wang, Hongzhou Yang, Yanmin Gao\*

School of Materials Science and Engineering, Jiangsu University of Science and Technology, Jiangsu, Zhenjiang 212003, China

\*E-mail: [JUSTGaoYanmin@163.com](mailto:JUSTGaoYanmin@163.com)

Received: 18 July 2020 / Accepted: 16 September 2020 / Published: 30 September 2020

In this paper, LiFePO<sub>4</sub>/C material was prepared by hydrothermal method. The effects of organic carbon source ascorbic acid, glucose and inorganic carbon source acetylene black on the properties of materials were studied. The specific capacity of the first discharge at 0.2C of the three kinds of carbon coated lithium iron phosphate reached 132.5mAh/g, 128.1mAh/g and 126.2mAh/g, respectively. Experiments show that the electrochemical performance of the LiFePO<sub>4</sub> coated with ascorbic acid is best. With ascorbic acid as the carbon source, when the addition amount of ascorbic acid was 5%, 7% and 10%, the first discharge specific capacity reached 132.5 m Ah/g, 156.9 m Ah/g and 130.8 m Ah/g, respectively. The results show that when the addition amount of ascorbic acid is 7%, the electrochemical performance is the best, reaching more than 90% of the theoretical capacity of LiFePO<sub>4</sub>. After 100 charge and discharge cycles at 0.2 C, the capacity retention rate is still 97.1%.

**Keyword:** Lithium-ion batteries; hydrothermal method; Carbon coating; FePO<sub>4</sub> precursor; LiFePO<sub>4</sub> positive electrode material

### 1. INTRODUCTION

With the deterioration of the progress of science and the environment, how to efficiently develop and utilize clean energy becomes a common challenge for mankind. As the representative of new clean energy, lithium ion battery has been developed rapidly in recent years. In 1983, Kim et al [1] discovered spinel crystal material with good conductivity as positive electrode material. By 2010, lithium ion battery (secondary battery, which can be charged and discharged for multiple times) has been widely used in industry, and has become the main energy source of electric vehicles [2]. At present, there are many types of lithium batteries, such as manganese acid lithium (LiMn<sub>2</sub>O<sub>4</sub>) [3], lithium nickel acid (LiNiO<sub>2</sub>) [4], lithium cobalt oxide (LiCoO<sub>2</sub>) [5] and lithium iron phosphate (LiFePO<sub>4</sub>).

As an important anode material in lithium batteries,  $\text{LiFePO}_4$  has low price, low environmental pollution, excellent thermal stability and structural stability (P-O covalent bond), and high theoretical specific capacity (170mAh/g) [6]. At present, it has become the preferred energy for portable electronic products and new energy vehicles. However, the low conductivity and slow diffusion coefficient of lithium iron phosphate restrict its development. Aiming at the problem of low electronic conductivity of lithium iron phosphate, we used different carbon sources [7] and different amounts of carbon sources to modify the synthesized  $\text{LiFePO}_4$  by carbon coating. Finally, the electrochemical performance of the improved  $\text{LiFePO}_4$  cell was the best when the amount of ascorbic acid was 7%.

## 2. EXPERIMENTAL

### 2.1. The preparation of $\text{FePO}_4$

Firstly, 4.04g  $\text{Fe}(\text{NO}_3)_3 \cdot 9\text{H}_2\text{O}$  was dissolved in 20ml deionized water to obtain solution A. Solution B was obtained by dissolving 1.15g  $\text{NH}_4\text{H}_2\text{PO}_4$  in 20ml deionized water. The solutions A and B were titrated slowly into the beaker, and fully stirred for 20 min before being transferred to the polytetrafluoroethylene reactor for hydrothermal reaction.  $\text{FePO}_4$  precursor was obtained after 6h reaction at  $120^\circ\text{C}$ .

### 2.2. The preparation of $\text{LiFePO}_4/\text{C}$

A certain amount of  $\text{FePO}_4$  and  $\text{Li}_2\text{CO}_3$  (molar ratio is 1:1.05) was weighed. Organic ascorbic acid (ASC), glucose (GLU) and inorganic carbon sources acetylene black (AB) were selected as carbon sources, and the samples were labeled as LFP/C-ASC, LFP/C-GLU and LFP/C-AB respectively. The carbon source added amount was 5%.

Place the fully mixed sample into a tubular furnace. First calcined at  $350^\circ\text{C}$  for 2h, then calcined at  $750^\circ\text{C}$  for 6h. Nitrogen atmosphere was always maintained in the sintering process, and the flow rate of  $\text{N}_2$  was 50ml/min. Finally,  $\text{LiFePO}_4/\text{C}$  positive electrode material was obtained.

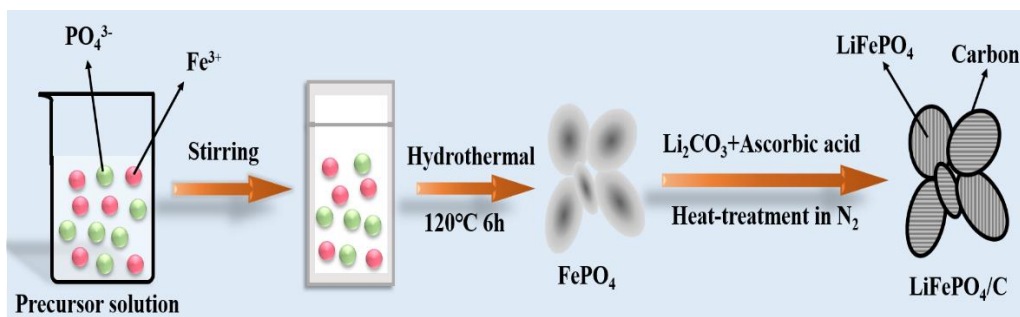


**Figure 1.** Preparation process of  $\text{LiFePO}_4/\text{C}$

## 2.2. The fabrication of Cells

LFP/C, Super P, and Polyvinylidene Fluoride (PVDF) were dissolved in N-methyl-2-pyrrolidone (NMP) in a weight ratio of 8:1:1. The mixed slurry was spread onto an aluminum foil current collector and dried at 60 °C under vacuum for 12 h. The model 2032 button battery was assembled in an argon filled glove box. The electrolyte was 1 M LiPF<sub>6</sub> in ethylene carbonate (EC) and diethyl carbonate (DEC) in a 1:1 v/v mixture of solvent

## 3. RESULTS AND DISCUSSION

### 3.1. Different carbon sources coated with lithium iron phosphate

#### 3.1.1 XRD

The LiFePO<sub>4</sub>/C positive electrodes synthesized from different carbon sources were characterized by XRD (Fig.2). Compared with pure phase LiFePO<sub>4</sub> [6], its diffraction peak is consistent with the standard spectrum. The absorption peaks of different samples are consistent with a larger peak, which is the diffraction peak of LiFePO<sub>4</sub>, and all have a single olivine structure. And the products coated by different carbon sources have no amorphous carbon diffraction peak [8]. This indicates that after the addition of a small amount of carbon sources, the residual carbon content on the surface or between particles after decomposition at high temperature is very small, which has limited effect on the crystal structure.

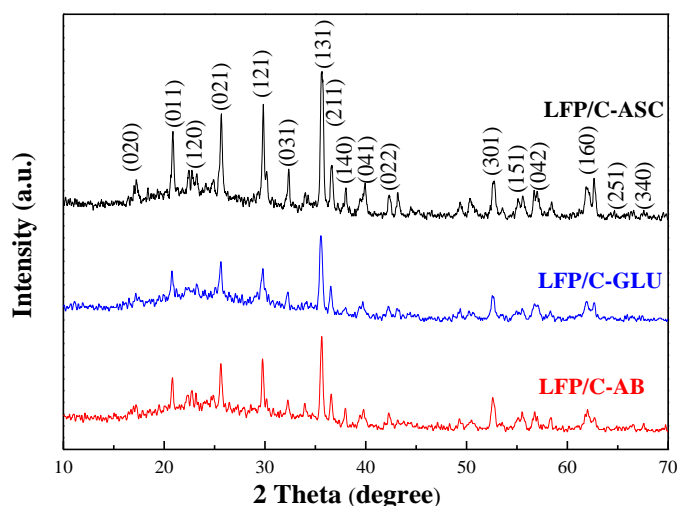


**Figure 2.** XRD characterization of LFP/C -ASC, LFP/ C-GLU, LFP/C-AB

#### 3.1.2 SEM morphology analysis

As can be seen from Fig.3. LiFePO<sub>4</sub> coated with different carbon sources showed no significant difference in morphology. All the three samples were formed by polymerization of small particles and secondary growth, and the crystal size was basically around 500-800nm. There is a certain gap between the small particles, which contributes to the transmission between lithium ions and facilitates the

diffusion of lithium ions, thus improving the crystallinity of  $\text{LiFePO}_4/\text{C}$  and reducing the vibration-density.

Ascorbic acid and acetylene black are both organic carbon sources, while Fig.3c is  $\text{LiFePO}_4$  coated with acetylene black from inorganic carbon source. As can be seen from Fig.3, the particle size of organic carbon source coated samples is better than that of inorganic carbon source coated samples. The particles are basically nanoscale to maintain the morphology of the precursor. At the same time, LFP/C-AB has certain agglomeration problems. Due to the effect of high temperature calcination, the grain growth is too fast. In the pre-sintering stage, the organic carbon source is carbonized into a viscous form and has relatively strong chelating ability to some transition metal elements, which finally makes the coating more uniform and the particles more finely dispersed [9].

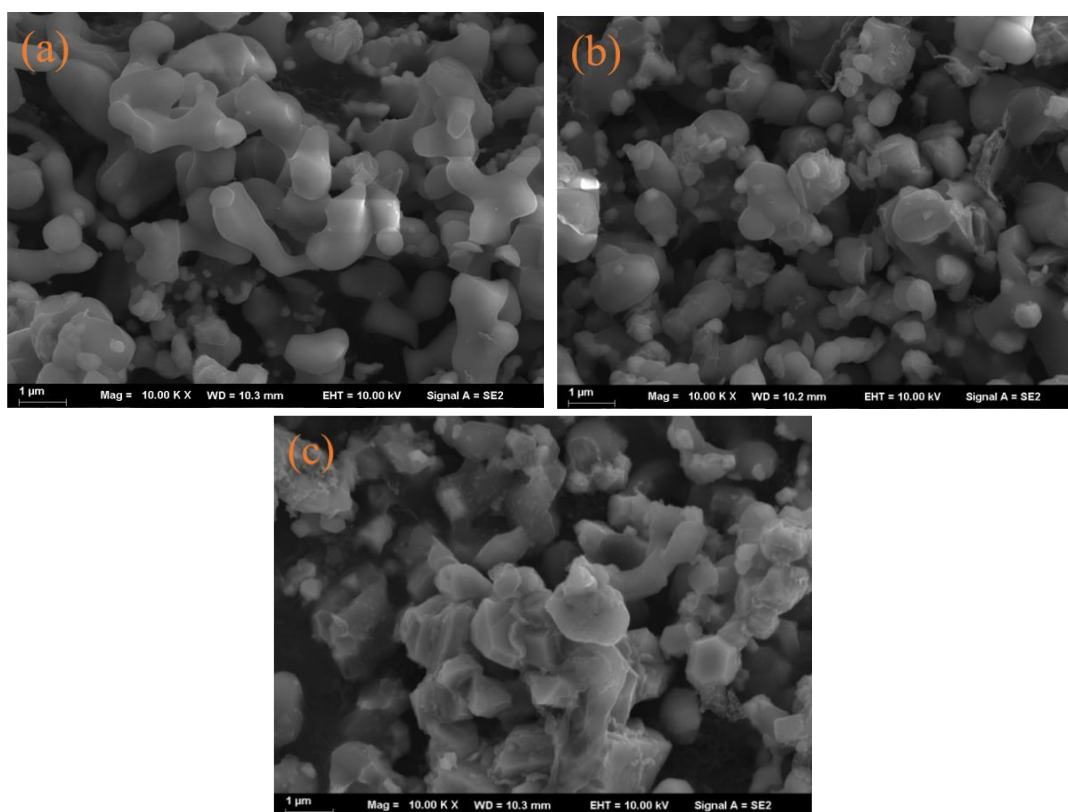
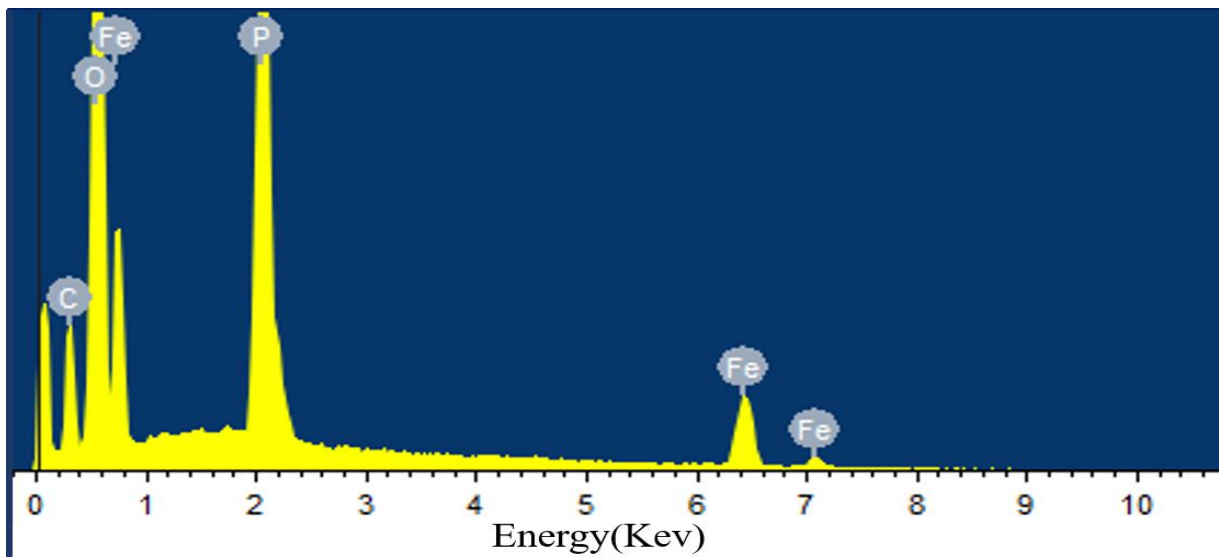


**Figure 3.** SEM images of  $\text{LiFePO}_4/\text{C}$  a) LFP/C-ASC; b) LFP/C-GLU; c) LFP/C-AB

**Table 1.** Ratio of elements in LFP/C-ASC

Element	Weight%	Atomic%
C	8.10	15.83
O	37.57	55.14
P	18.37	13.92
Fe	35.96	15.11

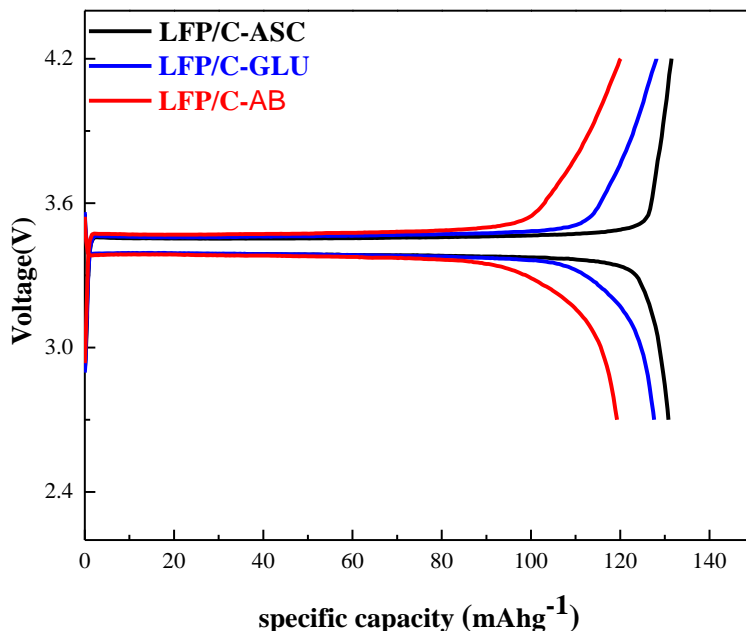
As can be seen from Table 1, the atomic percentage of element O is about four times that of P and Fe, which corresponds to the ratio of elements of chemical formula  $\text{LiFePO}_4$ . However, due to the low energy corresponding to Li in EDS energy spectrum, EDS cannot distinguish the presence of lithium element, so Li element does not appear in EDS. The atomic percentage of element C is 15.83%, which meets the requirement of carbon coating to synthesize  $\text{LiFePO}_4/\text{C}$ .



**Figure 4.** EDS images of LFP/C-ASC

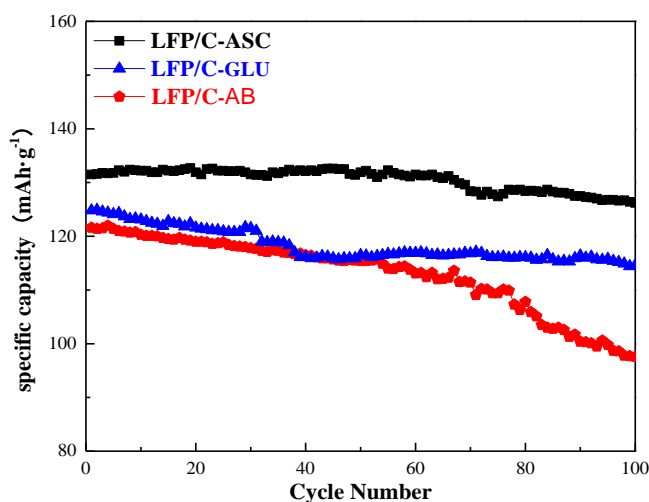
### 3.1.3 Analysis of electrochemical performance

Fig.5 shows the first charge and discharge capacity curve of  $\text{LiFePO}_4/\text{C}$ . The charging voltage platforms of three kinds of  $\text{LiFePO}_4/\text{C}$  composite materials are about 3.5V, and the discharging platform are 3.4V. The charging and discharging platforms of the materials are flat and slender, corresponding to the theoretical charging and discharging platform of  $\text{LiFePO}_4$ . The first discharge capacity of LFP/C – AB, LFP/C –GLU and LFP/C -ASC reached 120.1 m Ah/g, 128.1 m Ah/g, and 132.5 m Ah/g respectively. And the coulomb efficiency of LFP/C-ASC, LFP/C-GLU and LFP/C-AB reached 98.9%, 97.5% and 96.8%, respectively. The electrochemical performance of LFP/C-ASC is the best.



**Figure 5.** First charge and discharge capacity curve of LFP/C -ASC, LFP/ C-GLU, LFP/C-AB

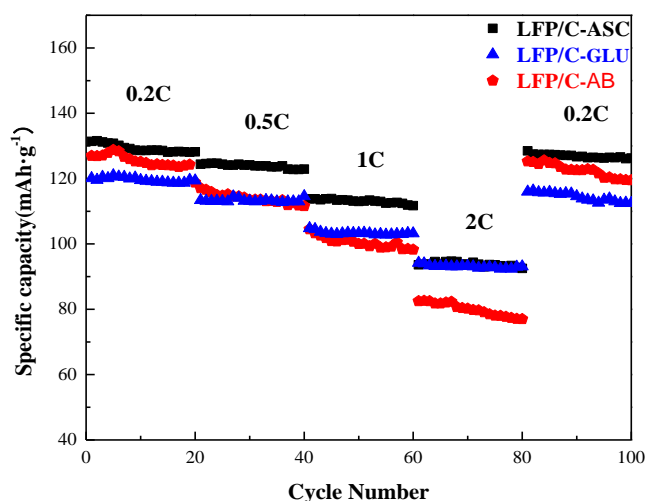
Fig.6 shows the cycle performance curve of  $\text{LiFePO}_4/\text{C}$  at 0.2C ratio. As can be seen from Fig.6, the cycling performance of LFP/C -ASC and LFP/ C-GLU is relatively excellent, while the cycling attenuation of LFP/C-AB is relatively fast. The first discharge specific volume of LFP/C-AB is 121.6m Ah/g, and the capacity after 100 cycles is 97.6m Ah/g. The capacity retention rate is only 80.3%. This is because acetylene black is an inorganic carbon source with low cracking temperature and residual carbon content, and less amorphous carbon content on the surface during cladding. This has a limited effect on material performance. After 100 cycles, the specific discharge capacity of LFP/ C-GLU decreases from 124.8mAh/g to 114.6mAh/g, and the capacity retention rate is around 91.8%. After 100 cycles, the specific discharge capacity of LFP/C -ASC is reduced from 132.5mah /g to 126.2mah /g, with a capacity retention rate of 95.9%. This indicates that LFP/C -ASC has the best cycling performance.



**Figure 6.** Cycle performance curve of LFP/C -ASC, LFP/ C-GLU, LFP/C-AB

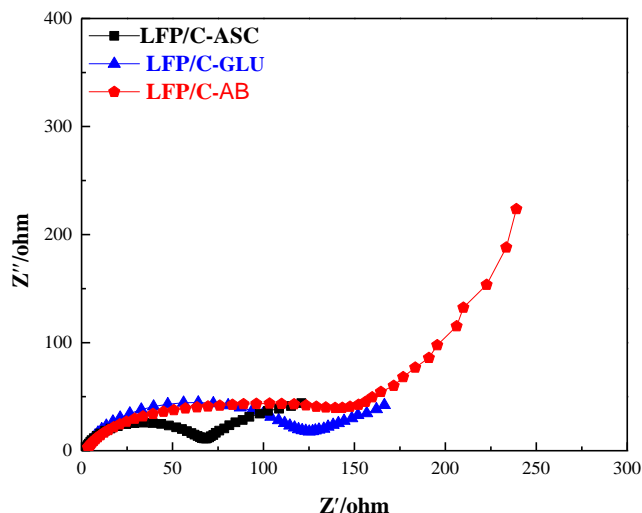
Fig.7 shows the cycling performance of  $\text{LiFePO}_4/\text{C}$  at different rate. We can see that LFP/C -ASC, LFP/ C-GLU and LFP/C-AB all have relatively good cycling performance. Under the same ratio, discharge curve is substantially stable state.

When LFP/ C-GLU and LFP/C-AB discharge at 0.5C and 1C, there is little difference in discharge specific capacity. However, under the 2C discharge ratio, LFP/C-AB experienced a sudden drop. LFP/C -ASC and LFP/ C-GLU are lithium iron phosphate coated with organic carbon sources. The organic carbon source has a large molecular weight and will remain more carbon after calcination. The residual carbon can better cover the surface of  $\text{LiFePO}_4$ , thus inhibiting the growth of particles. At the same time, organic gas may be produced and continue to accumulate on the surface. However, acetylene black and  $\text{LiFePO}_4$  are only pure physical mixing and cannot fully contact  $\text{LiFePO}_4$  particles, resulting in incomplete coating [10]. With the increase of discharge ratio, the specific discharge capacity of LFP/C -ASC sample has hardly decreased, and it can still reach 128.5m Ah/g.



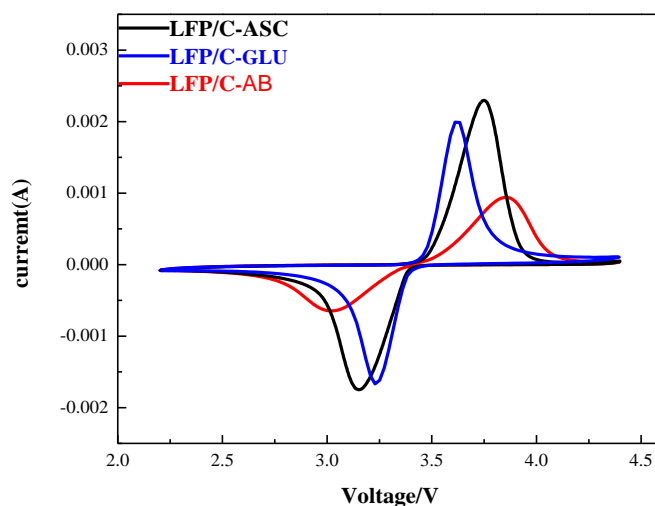
**Figure 7.** Cyclic performance curves of LFP/C -ASC, LFP/ C-GLU, LFP/C-AB at different rates

Fig.8 is the electrochemical impedance spectral of  $\text{LiFePO}_4/\text{C}$ . The alternating current frequency is from 10 kHz to 0.01Hz, and the amplitude is 5mV. From Fig.8, we can see that the electrochemical impedance spectral of all three samples consist of a semicircle in the high frequency region and a straight line in the low frequency region. The semicircle represents the charge transfer process, and the diagonal line represents the lithium ion Warburg diffusion process. The semicircle radius of LFP/C -ASC is the smallest, indicating that the addition of ascorbic acid can reduce the electrode over-potential and battery polarization, thus improving its cycling performance and specific discharge capacity. LFP/C-AB has the largest impedance radius, indicating poor dynamic performance and strong polarization, which will eventually lead to poor cycling performance and power reduction performance at high magnification.



**Figure 8.** Electrochemical impedance spectral of LFP/C -ASC, LFP/ C-GLU, LFP/C-AB

Fig.9 shows the cyclic voltammetry of LiFePO<sub>4</sub>/C. The scanning speed was 0.1mv /s and the scanning range was 2.2V-4.4V. Among them, LFP/C-ASC has the largest peak area, the sharpest redox peak, and excellent cycling reversibility. This indicates that the polarization of the material is not obvious when coated with ascorbic acid. Therefore, using ascorbic acid as carbon source can improve the decoupling ability of lithium ions and the reversibility of batteries.



**Figure 9.** Cyclic voltammetry of LFP/C -ASC, LFP/ C-GLU, LFP/C-AB

Based on the phase analysis, structural analysis and electrochemical performance analysis of LFP/C -ASC, LFP/ C-GLU and LFP/C-AB, we have concluded that coating LiFePO<sub>4</sub> with ascorbic acid can effectively improve the morphology and size of the material, increase the initial specific capacity of the material, and improve the performance of the battery. Therefore, in this article, we will use ascorbic



acid as the carbon source to study the effect of carbon content on the electrochemical performance of materials.

### 3.2. Electrochemical analysis of different carbon contents

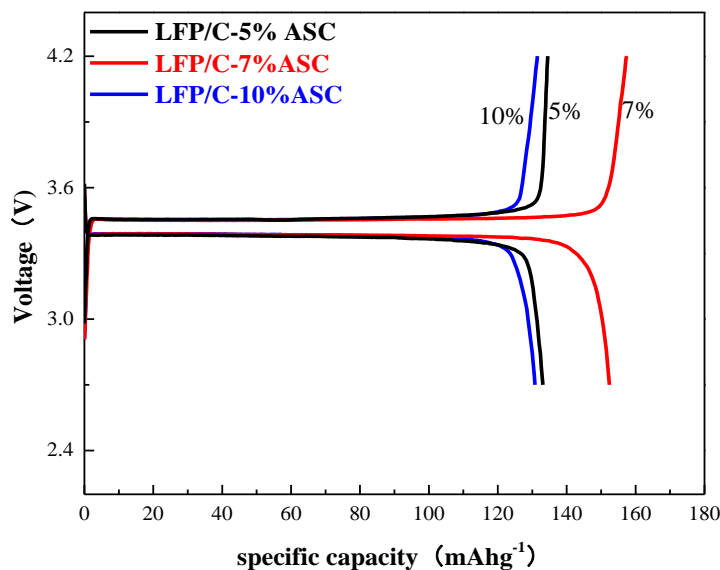


**Figure 10.** First charge and discharge curve of LFP/C -5%ASC, -7%ASC, -10%ASC at 0.2C

As can be seen from Fig.10, the discharge platforms of  $\text{LiFePO}_4/\text{C}$  with different addition of ascorbic acid are around 3.40V, which is consistent with the theoretical discharge platform of  $\text{LiFePO}_4$ . When the ascorbic acid content is 5%, 7%, and 10%, the first discharge capacity reached 132.5mAh/g, 156.9mAh/g, and 130.8mAh/g, respectively. The discharge capacity of LFP/C -7%ASC reached 92.1% of  $\text{LiFePO}_4$  theoretical specific capacity. When the carbon content is 5%, due to the insufficient carbon content, the coating of the material surface was not complete. When sintered at high temperature, the amount of carbon can't restore all of the ferric iron, resulting in limited improvement in material properties [11]. When the carbon content is 10%, as can be seen from the SEM figure that the particle size of the material is large and there is a little agglomeration phenomenon, which affects the transfer rate of lithium ion. When carbon content is excessive,  $\text{Fe}_2\text{P}$  impurity phase may be formed, which will affect its final electrochemical performance.

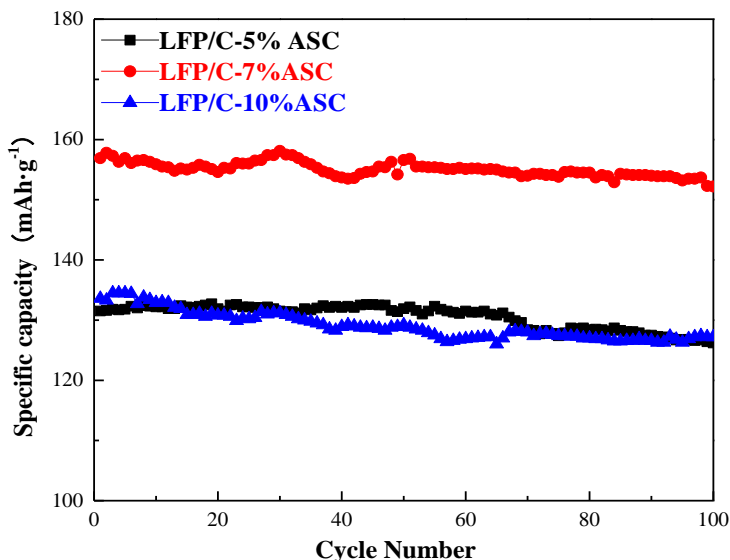


Figure 11. Cyclic performance of LFP/C -5%ASC, -7%ASC, -10%ASC at 0.2C

As can be seen from Fig.11, the specific capacity of LFP/C -5%ASC decreases from 132.5mAh/g to 127.2mAh/g, and the capacity retention rate is 95.5%. When the addition amount is 10%, after 100 cycles, the specific capacity of LFP/C -10%ASC is reduced from 130.8mAh/g to 126.2mAh/g, and the capacity retention rate is 96.4%. When ascorbic acid is added at 7%, its initial capacity is 156.9mAh/g. After 100 cycles, the capacity is still up to 152.2mAh/g. And the capacity retention rate is 97.1%.

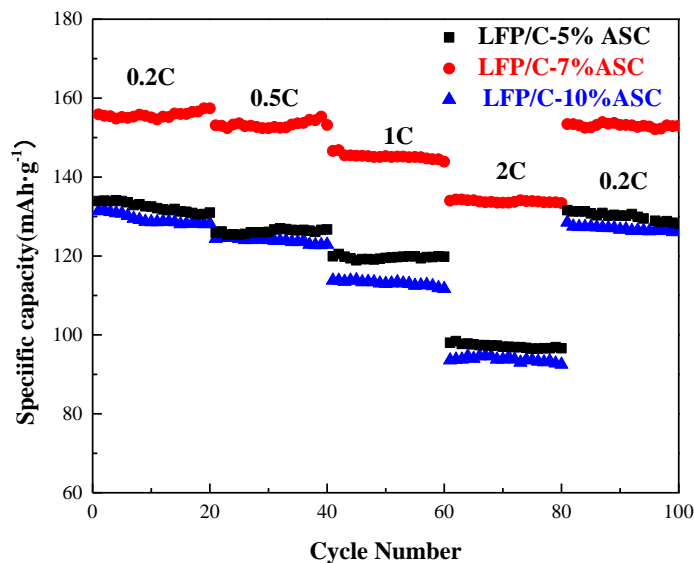
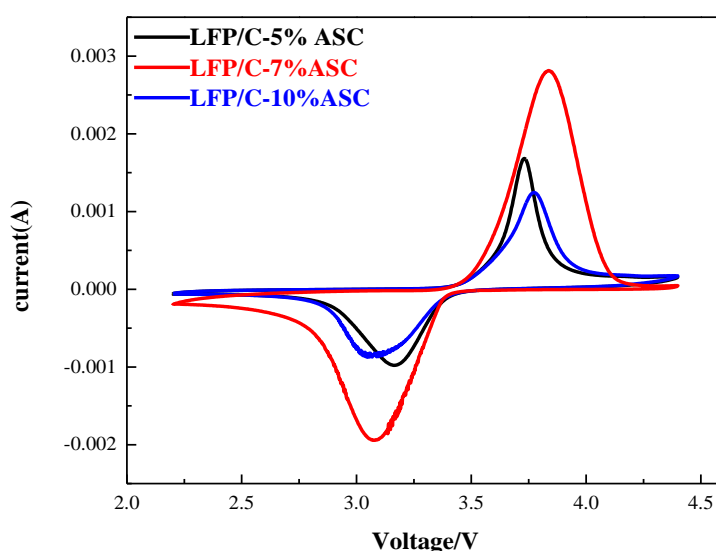


Figure 12. Cyclic performance curves of LFP/C -5%ASC, -7%ASC, -10%ASC at different discharge rates

As can be seen from Fig.12, with different carbon content, the discharge specific capacity varies greatly in different rate. The specific capacity and change trend of LFP/C -5%ASC and LFP/C -10%ASC are almost the same, but the curve of LFP/C -10%ASC decreases slightly at 1C ratio. This is because after a period of constant electric discharge, the excessive carbon layer on the surface obstructs the migration of lithium ions and reduces the diffusion rate of lithium ions. The specific capacities of LFP/C -7%ASC under 0.2C, 0.5C, 1C and 2C are 156.9mAh/g, 152.7mAh/g, 145.3mAh/g and 134.1mAh/g, respectively. In the same rate discharge process, the curve is flat and the specific capacity hardly decreases. After 2C high current charging and discharging, the specific capacity can still reach 153.1mAh/g at 0.2C. It shows excellent multiplier characteristics and electrochemical performance. According to relevant reports, the initial discharge specific capacity of the materials prepared by Liu et al at 0.1 C is 152.5 mAh/g [12].



**Figure 13.** Cyclic voltammetry of LFP/C -5%ASC, -7%ASC, -10%ASC

As can be seen from Fig.13, the peak area and the redox peak of LFP/C -10%ASC are small. This is because the carbon layer thickness increases due to the excessive carbon content, hindered the lithium ions embedded ability, resulting in a decline in ion diffusion rate and reversibility. LFP/C -7%ASC has the largest peak, indicating that the specific capacity is also the largest. Moreover, the symmetry of the peak is excellent, which indicates that the material has good reversibility.

#### 4. CONCLUSIONS

In this paper, lithium iron phosphate was coated with ascorbic acid, glucose and acetylene black, and the following conclusions were drawn: LFP/C-ASC has good morphology, and the specific discharge capacity reaches 132.5mAh / g for the first time. With ascorbic acid as the carbon source,

when the ascorbic acid content is 5%, 7% and 10%, the first discharge specific capacity is 132.5 m Ah/g, 156.9 m Ah/g and 130.8 m Ah/g, respectively. The results show that when addition amount of ascorbic acid is 7%, the electrochemical performance is the best, reaching more than 90% of the theoretical capacity of LiFePO<sub>4</sub>. After 100 charge and discharge cycles at 0.2 C, the capacity retention rate is still 97.1%.

## References

1. JB Goodenough, Y Kim, *JACS*, 22 (2009) 587-603.
2. D Ansean, M Gonzalez, J C Viera, *IEEE Trans. Ind. Appl.*, 51(2015).
3. WIF David, MM Thackeray, PG Bruce, *Mater. Res. Bull.*, 19 (1984) 99-106.
4. A. Hirano, K. Kanie, T. Ichikawa, *Solid State Ionics*, 152 (2002) 207-216.
5. S. H. Park, Y. Sun, K. S. Park, *Electrochim. Acta.*, 47.11 (2002) 1721-1726.
6. J Chen, S Wang, M S Whittingham, *J. Power Sources*, 174.2 (2007) 442-448.
7. C Gong, Z Xue, S Wen, *J. Power Sources*, 318(2016) 93-112.
8. X Fan, J Luo, C Shao, X Zhou, Z Niu, *Electrochim. Acta.*, 158 (2015) 342-347.
9. H Meng, B Wang, L Han, *New Chemical Materials*, 7 (2016) 171-174.
10. C Gong, Z Xue, S Wen, *J. Power Sources*, 318 (2016) 93-112.
11. F Pignanelli, M Romero, D Mombrú, *Ionics*. 25 (2019) 3593-3601.
12. Z Liu, Y Zhu, P Gao, *Int. J. Appl. Ceram. Technol.*, 17.3(2020) 1231-1240.

© 2020 The Authors. Published by ESG ([www.electrochemsci.org](http://www.electrochemsci.org)). This article is an open access article distributed under the terms and conditions of the Creative Commons Attribution license (<http://creativecommons.org/licenses/by/4.0/>).